INFLUENCE OF A DETAILED MASS ESTIMATION FOR A WING WITH KNOWN FLIGHT SHAPE IN CONCEPTUAL OVERALL AIRCRAFT DESIGN

T. Effing*, R. Stephan*, E. Stumpf*
* Institute of Aerospace Systems (ILR), RWTH Aachen University, Wüllnerstraße 7, 52062 Aachen, Germany

Abstract

In the conceptual stage, a detailed wing mass estimation is crucial to map the influence of geometric wing changes or the integration of new technologies on the overall aircraft design. Before, the conceptual aircraft design environment MICADO used a known flight shape of the wing for aerodynamic analyses; the wing mass was estimated with semi-empirical methods without any aeroelastic coupling. This work presents results from advancements towards integrating existing methods from literature for a detailed wing mass estimation into MICADO, made in the last years. Besides a more detailed wing mass estimation, these methods enable, e.g., the consideration of the impact of the lift distribution on the wing mass by coupling aerodynamic and structural effects for different load cases. Since the applied methods for dimensioning the wing box require a jig shape, it is inversely calculated if only the flight shape is known beforehand. Hence, the process is independent of the given (jig or flight) shape of the wing. After presenting the new module, selected application studies demonstrate the new capabilities of MICADO. For the short-medium range aircraft used in the studies, the results indicate that creating flexible wing polars with lift-dependent flight shapes only slightly influences the final results of an overall aircraft design. Similarly, it is demonstrated that an aircraft with variable camber (VC) application exhibits—from an overall aircraft design perspective—minor differences in the flight shape and, thus, in the aerodynamic performance when flaps are deployed, compared to a rigid configuration. However, the impact on aerodynamics and structures is significant when designing aircraft with different target lift distributions. From these findings, application guidelines are derived for the aircraft range type used within this work. In future studies, these design guidelines can be assessed for different aircraft range types and eventually generalized.

Keywords

Conceptual aircraft design; wing mass estimation; short-medium range aircraft

1. INTRODUCTION

In recent years, the assessment of wing aerodynamics in the conceptual aircraft design environment MICADO[1] has been improved, e.g., to evaluate new technology options such as hybrid laminar flow control and variable camber (VC) [4–7]. Previously, the MICADO process chain, as shown in Fig. 1, used a known rigid flight shape of the wing for aerodynamic analyses; the wing mass was estimated with semi-empirical methods [8, 9] without any aeroelastic coupling. In cases where the wing mass data of the reference aircraft designs were known in advance, the results were calibrated.

Since recent developments focused on improving the prediction of aerodynamic key parameters, a new wing mass estimation module was developed in order to maintain the interdisciplinary balance between tool complexity and accuracy required for a consistent conceptual design environment.

This paper presents the results of progress made in recent years towards the integration of existing methods from the literature [10–13] for a more detailed wing mass estimation in MICADO. The adapted methodology from the literature targets to calculate the wing mass more precisely and consists of an iterative aerostructural process, which considers different load cases. Starting with the input of the jig shape, the iterative approach ensures that the deformed wing shape and the aerodynamics loads align. Finally, the wing mass is derived based on the dimensioned wing box structure. Besides the more detailed wing mass estimation, these methods allow, e.g., to consider the influence of the lift distribution on the wing mass by coupling aerodynamic and structural effects for different load cases. Since the applied methods require a jig[2] shape for dimensioning the wing box, it is calculated inversely if only the flight shape is known in advance. Therefore, the procedure is independent of the given shape, jig or flight, of the wing.

[1] Multidisciplinary Integrated Conceptual Aircraft Design and Optimization environment [1, 2]; MICADO is an internal specialization of UNICADO [3] providing selected methods with higher fidelity.

2. METHODOLOGY FOR A DETAILED MASS ESTIMATION

This chapter discusses the wing mass estimation methodology, as shown in Fig. 2, within the context of the MICADO aircraft design process (Fig. 1). This estimation is conducted as part of the design analysis phase. First, the process description focuses on how the methodology operates when provided with a predetermined wing jig shape, consistent with methods established in the existing literature. Second, attention is given to how the calculation can be adapted when the flight shape is known beforehand instead of the jig shape.

2.1. Wing mass calculation with known jig shape

This section addresses the wing mass estimation for a given jig shape, as indicated by the blue arrows in Fig. 2, representing the first option of the process chain. Implementation details are given by Wecker [14], with an extensive overview of the references.

[2] The jig shape refers to the wing geometry without aerodynamic loads acting upon it.

doi: 10.25967/610340

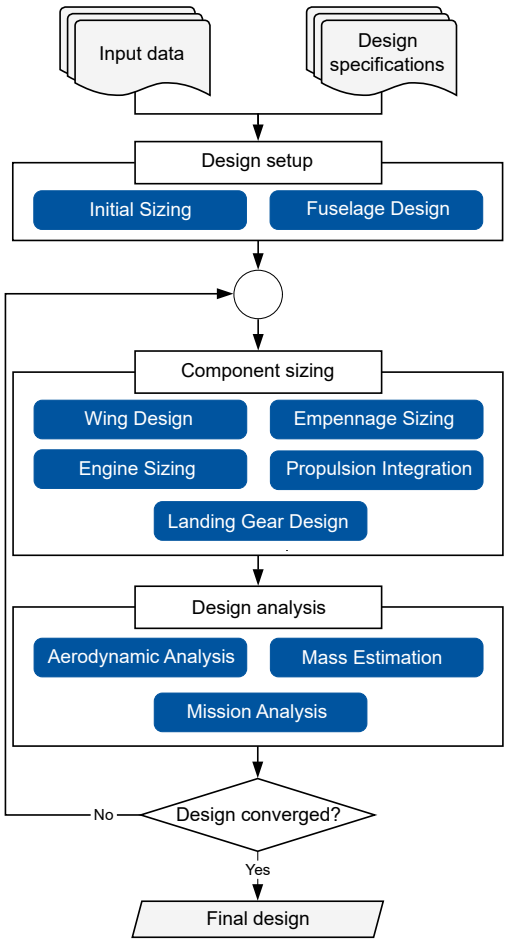

FIG 1. MICADO process

The core of the methodology is the dimensioning of the wing box, with a simplification reducing the wing box to dimensions of skin and web thicknesses [10], both assigned with an initial assumption for the thickness. Out of several existing load cases [13], three load cases are identified as dimensioning [10, 14]: a 2.5-g pull-up maneuver, a vertical gust, and a roll maneuver. An aeroelastic convergence loop [13], called the inner loop, is initiated for each load case. The aerodynamic loads are first calculated in the inner loop by applying the Athena Vortex Lattice (AVL) program [15] to the jig shape. The results are then passed to a structural finite element (FEM) analysis. Here, the wing is divided into structural nodes, each of which is assigned a wing box thickness for the web and skin with a minimum value of $0.5\,\mathrm{mm}$ for both. This aerostructural coupling results in a deflected wing geometry that requires subsequent iterative aerodynamic and structural recalculation. After the inner loop converges, the wing box dimensions for the skin and web are known for one load case. After performing this inner loop for each load case, the wing box web and skin dimensions are aggregated.

Finally, the 1-g cruise flight calculations are performed based on the dimensioned wing box. This geometry and the total wing mass determined from the wing box and other structural elements are then returned to the MICADO design process chain.

Another viable option for application is available when the jig shape and wing box dimensions are already known in advance. In that case, the geometry preparation and the inner loop can be omitted, allowing for direct calculations of the flight shape and the overall wing mass.

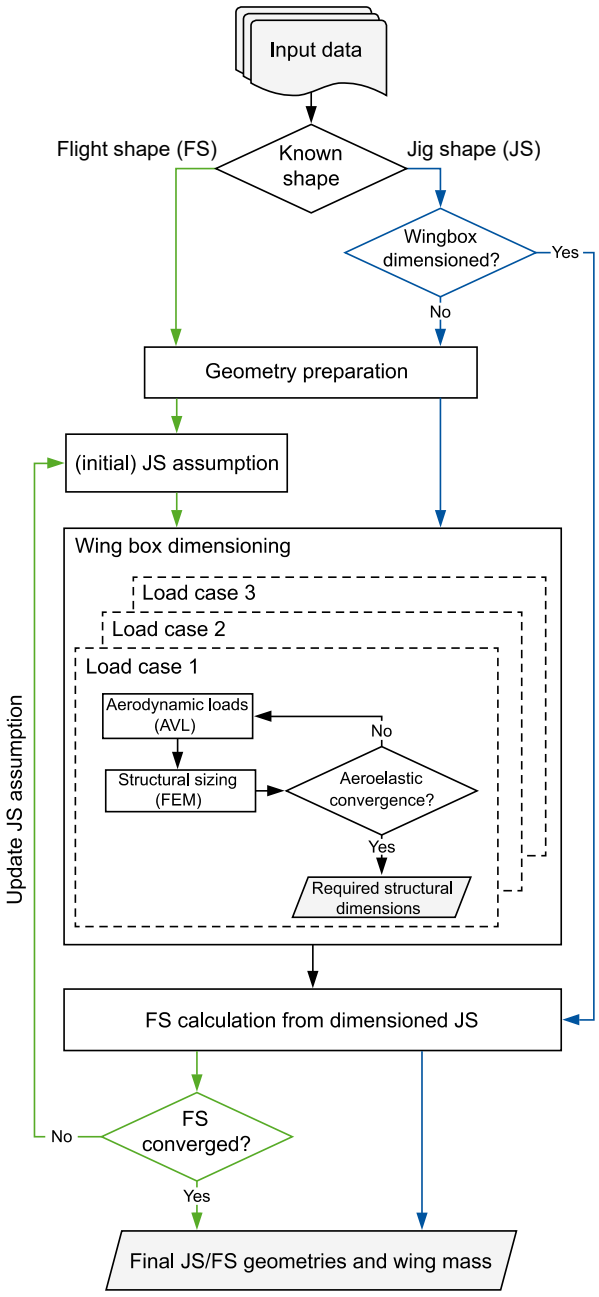

FIG 2. Wing dimensioning process chain

2.2. Wing mass calculation with known flight shape

When the flight shape of the wing is provided as input, an additional process step, indicated by the green arrows in Fig. 2, is required since the basic methodology is initially designed for a known jig shape. Following the geometry preparation step, an initial jig shape assumption is required to apply the wing box dimensioning described in Sec. 2.1. Preliminary investigations have shown that this initial jig shape assumption can be kept relatively coarse due to the rapid convergence of the subsequent iterative process.

With this initial jig shape assumption, the wing box dimensioning process is performed, resulting in an initial flight shape estimation. This flight shape is then compared to the

input geometry with the target flight shape, and adjustments to the assumed jig shape are made accordingly [11]. This iterative process evaluates the convergence of the vertical deflections and twist angles, allowing a maximum deviation of $0.1\,\mathrm{m}$ and 0.1°, respectively, between the target and calculated flight shapes.
The options presented here provide a versatile approach that primarily offers the capability to calculate the mass of the wing for a given flight or jig shape in a more sophisticated manner than is available with conventional handbook methods. Furthermore, calculations can be performed, e.g., for a single baseline wing under different loading conditions, such as different lift coefficients or in cases with variable camber applications. The computation time varies depending on the specific case but is typically on the magnitude of seconds. Since wing mass estimation is an integrated part of a more extensive iterative aircraft design process, it is essential to maintain reasonable computation times without excessive delays for single tools in the overall design chain.

3. APPLICATION

This chapter presents several application studies using the new capabilities of MICADO. In Sec. 3.1, the short-medium range reference aircraft is briefly described. Afterwards, the following specific questions are answered:

- **Sec. 3.2**: How does a sophisticated flight shape consideration impact the overall aircraft design results?
- **Sec. 3.3**: How does integrating the variable camber technology influence the design process when the corresponding wing deformations are correctly mapped?
- **Sec. 3.4**: How significantly do different lift distributions influence the aircraft design?

3.1. Reference design

For the reference aircraft, a CS-25 short-medium range reference aircraft is used. This aircraft is a derivative from the CeRAS[3] short-range reference aircraft, representing an aircraft similar to an Airbus A320neo. It was designed with the MICADO process from Fig. 1. Note that the new wing mass estimation module was used with, in this case, a given FS. Hence, the JS was determined iteratively using the process chain highlighted in green in Fig. 2.
Figure 3 shows the segmented wing planform of the reference aircraft, which has a span of roughly $36\,\mathrm{m}$ and a reference area of $127\,\mathrm{m}^2$. In addition, the control device setup, relevant for the study case with integrated variable camber (VC) technology in Sec. 3.3, is illustrated.

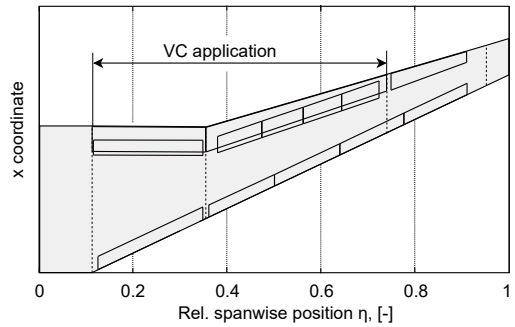

FIG 3. Wing planform with control device layout of the reference aircraft

[3]The "Central Reference Aircaft data System" database provides reference aircraft data for public access and enables communication within the research community [16, 17].

For the converged reference aircraft, Figure 4 shows the mission altitude profile with one step climb and the associated sawtooth-like contour of the global lift coefficient $\mathrm{C_L}$.

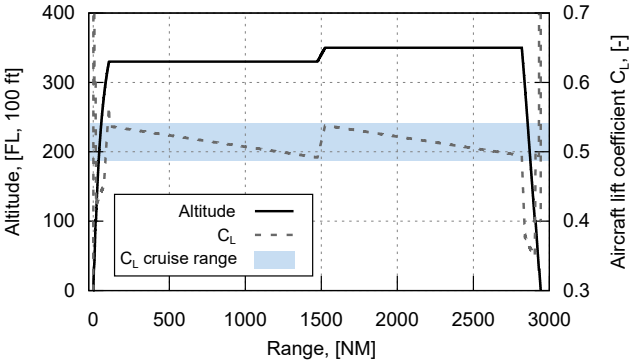

FIG 4. Altitude and lift coefficient profiles for the reference aircraft

The resulting 3D aircraft geometry is illustrated in Fig. 5; relevant input and output design parameters are listed in Tab. 1.

FIG 5. 3D aircraft geometry of reference aircraft

TAB 1. Key parameters of short-medium range reference aircraft

Parameter	Unit	Value
Initial cruise altitude	ft	33 000
Cruise Mach number	-	0.78
Maximum take-off mass (MTOM)	t	79.0
Operating empty mass (OEM)	t	45.0
Wing mass ($\mathrm{m_{wing}}$)	t	8.9
Tripfuel design mission ($\mathrm{TF_{2943\,NM}}$)	t	14.5
Opt. lift-to-drag ratio ($(\mathrm{L/D})_{\mathrm{opt}}$)	-	17.7

3.2. Analysis of different flight shapes per lift coefficient

This study aims to identify the impact of a more sophisticated flight shape consideration on overall aircraft design results. Therefore, instead of using only the design flight shape, wing shape permutations are calculated for every lift coefficient during trimmed steady cruise flight; these are highlighted in blue in Fig. 4. Applying a sufficient safety margin, flight shapes are calculated for $0.45 \leq \mathrm{C_L} \leq 0.6$ with a step width of $\Delta \mathrm{C_L} = 0.025$. The resulting deformations for the minimum and maximum lift coefficient in steady cruise flight are shown in Fig. 6. Additionally, the calculation approach, i.e., the different modes of the new wing mass estimation module, is depicted in the upper box using the same color coding as in Fig. 2.

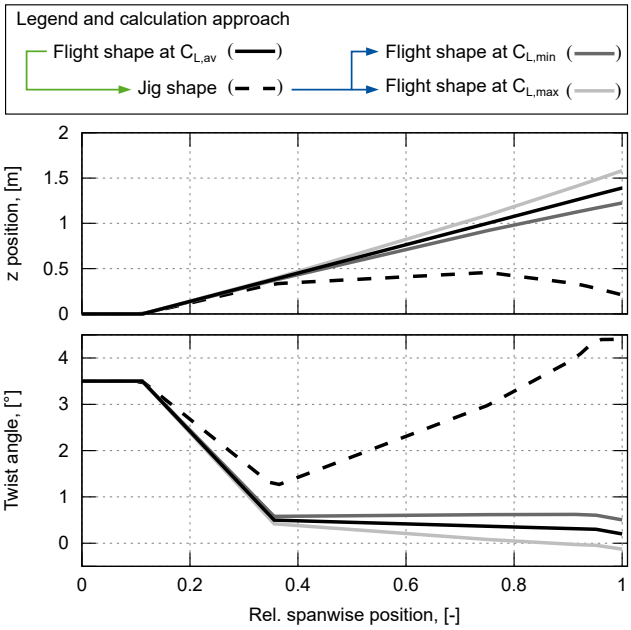

FIG 6. Calculated wing deformations in cruise flight range

As highlighted in the upper box, the calculation starts with iteratively determining the jig shape, i.e., both vertical z position and twist angle deflection, from the given flight shape at the average lift coefficient in cruise. Afterward, the lift-dependent flight shapes are calculated using the previously derived jig shape and the respective structural wing box dimensions.

Compared to the reference case with a single rigid flight shape (solid black lines), the mission-variable flight shapes yield slightly higher twist values (and less vertical deflection) at the tip for lower lift coefficients (dark grey lines). The effects for higher lift coefficients are vice versa (light grey lines). The different shapes are then used to derive a flexible wing polar by analyzing the aerodynamics and merging the lift-to-drag polars for every lift coefficient. The lift polars for $\mathrm{C_{L,min}}$ and $\mathrm{C_{L,max}}$ are also used for the range below or above the addressed $\mathrm{C_L}$ range; note that this is mainly for visualization, as the corresponding values are irrelevant during cruise flight. The resulting lift-to-drag polars are shown in Fig. 7.

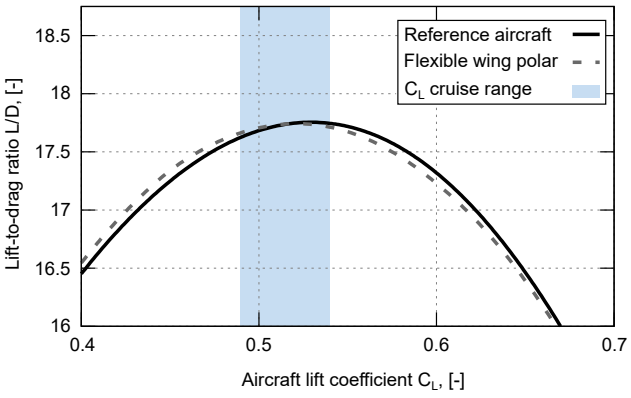

FIG 7. L/D polars for both the aircraft with a rigid and a flexible wing

It can be seen that considering different wing shapes per lift coefficient leads to deviations in the $\mathrm{L/D}$, with the largest differences at the boundaries of the considered $\mathrm{C_L}$ range. The deviations are due to altered lift distributions and the corresponding changes in drag coefficients. However, the deviations are comparably minor for the lift coefficients relevant for steady cruise flight. Replacing the aerodynamics from the reference aircraft with the flexible wing polar, the analysis of the design mission leads to a difference in required trip fuel of $\Delta \mathrm{TF}_{2943\,\mathrm{NM}} < 5\,\mathrm{kg}$. This negligible difference can be traced back to the small aerodynamic differences within the $\mathrm{C_L}$ cruise range, again highlighted in blue in Fig. 7.

To summarize, for the aircraft type at hand, the increased effort to create the different flight shapes and the respective flexible wing polar is not recommended since almost no impact is detected on the overall aircraft design level; the change in mission fuel consumption is negligible.

3.3. Influence of different flight shapes for VC application

Based on the findings of the previous section, this study aims to investigate the potential influence of a more advanced wing shape calculation method in the context of a variable camber (VC) application. Specifically, both high-lift flaps shown in Fig. 3 are allowed to be deflected between $-3°$ and $4°$ during cruise flight while using the spoiler to close the opening gap for performance optimization.

This investigation focuses on comparing the VC polar derived from a rigid flight shape with one derived from a flexible flight shape. The methodology for VC studies is introduced by Peter [4] and was subsequently applied, e.g., in Refs. [6,7]. It consists of the aerodynamic computation of all possible flap setting permutations. Subsequently, the $\mathrm{L/D}$ polars of all wing permutations are merged into one VC polar; this is done based on the best lift-to-drag ratio for every polar point.

For the rigid wing, each permutation is based on the same flight shape. In contrast, for the flexible wing, a new flight shape is calculated for each flap setting permutation. Both variants share a similar jig shape. The resulting wing shapes are visualized in Fig. 8 for the average lift coefficient $\mathrm{C_L} = 0.51$ and the specific flap setting $1°$ on the inboard flap and $4°$ on the outboard flap.

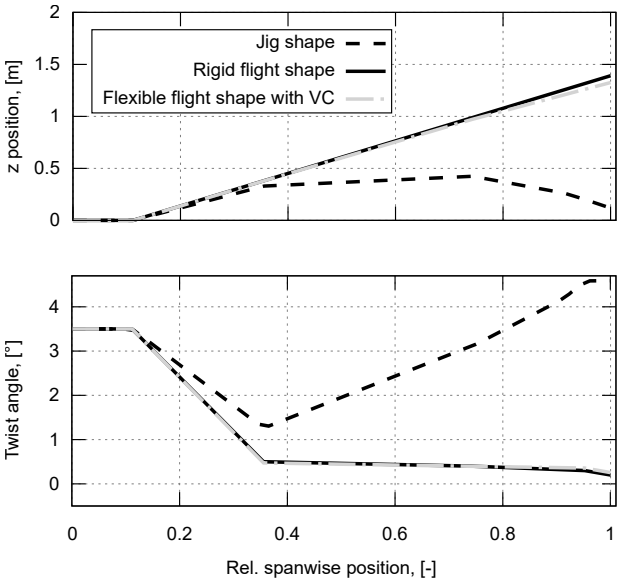

FIG 8. Wing shapes for both the aircraft with a rigid and a flexible wing in the VC setting 1° inboard and 4° outboard

Although the changes in dihedral and twist are small, they are noticeable. The flexible wing has a slightly lower dihe-

dral but a higher twist, especially towards the outboard region.
The modified wing geometries produce different aerodynamic results as illustrated in the $\mathrm{L/D}$ polar in the upper part of Fig. 9; in the middle and lower parts of the figure, the deflections of the inboard and output flap, respectively, are shown.

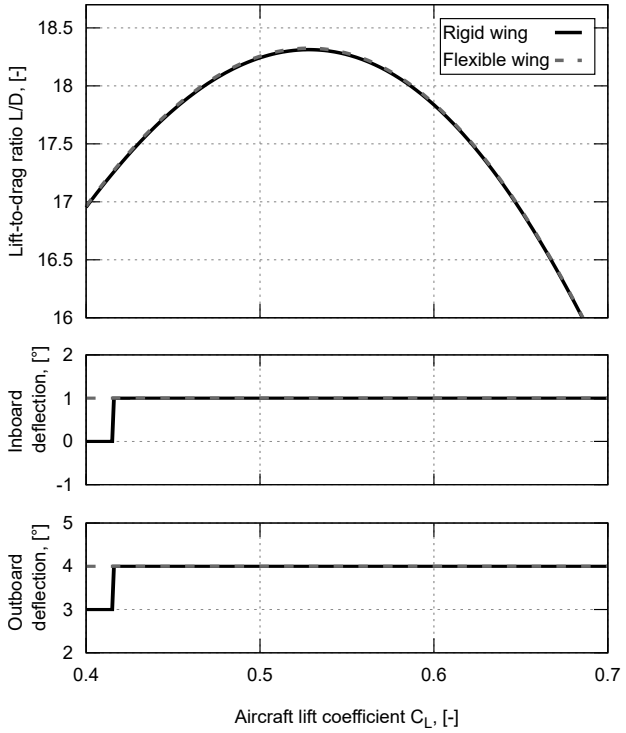

FIG 9. L/D polars with a VC application for both the aircraft with a rigid and a flexible wing

Over the range of cruise lift coefficients, the flexible wing shape results in a slight increase in $\mathrm{L/D}$. Since the flap deflections remain almost the same throughout the mission, the qualitative effects are unchanged.
However, these effects are considered negligible in the context of the conceptual aircraft design. The considerations result in only a small change in trip fuel consumption of $\Delta \mathrm{TF}_{2943\,\mathrm{NM}} < 2\,\mathrm{kg}$, which is way below the set convergence criterion of $\epsilon \leq 10^{-4}$ in MICADO.
In summary, the flexible wing effects are observed in an illustrative VC application but do not affect the results sufficiently to justify the additional effort in future applications. In addition, neglecting the effects ignores the slight increases in $\mathrm{L/D}$ and, thus, provides a conservative estimate.

3.4. Analysis of the impact of different lift distributions

This final study presents the impact of different lift distributions on the overall aircraft design. Before, such a study could only predict the influence on the aerodynamics. Due to the capabilities introduced with the new wing mass estimation module, the influence on the wing structures can now be considered. In addition to the reference aircraft, two other aircraft are designed for this study. Using another MICADO module for automatically adjusting the twist distribution [18], an elliptical and a bell-shaped lift distribution are targeted during the design loop. The resulting lift distributions for a wing lift coefficient of $\mathrm{C_{L,wing}} = 0.5$ are shown in Fig. 10.
Each wing with its adjusted twist is considered a separate, known flight shape to analyze the impact of the different lift distributions on the wing dimensioning process. Hence,

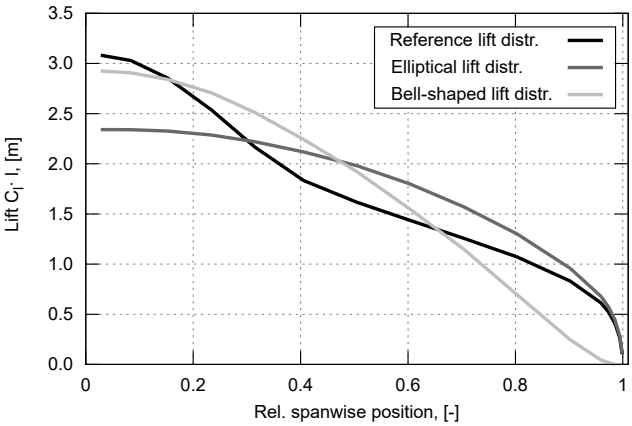

FIG 10. Predefined lift distributions of case study aircraft

contrary to the previous studies, three different target flight shapes are used as a starting point for the process chain highlighted in green from Fig. 2. The changes in local lift and the associated shift of the center of pressure are tracked in the process and lead to unique jig shapes and dimensioned wing boxes for each case; the calculated masses are subsequently fed back to the MICADO design loop. The resulting jig shapes of the different aircraft (AC) alongside their respective target flight shapes are illustrated in Fig. 11.

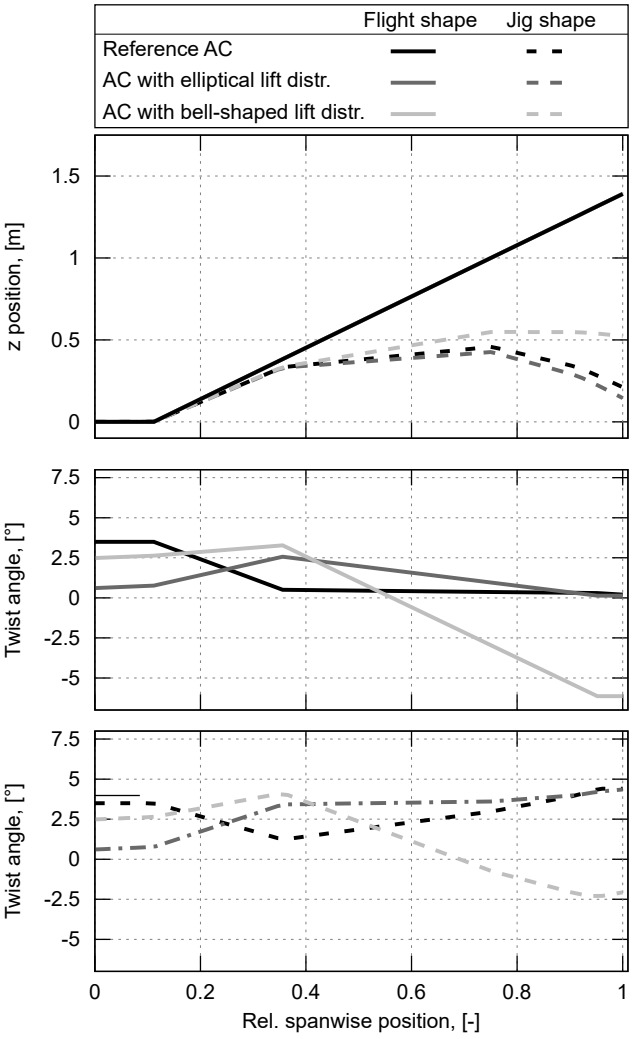

FIG 11. Wing deformations due to different lift distributions. Upper part: z deflection (FS and JS); middle part: twist distr. (FS); lower part: twist distr. (JS)

Note that all three study aircraft share the same z deflection in flight shape (solid lines in the upper part) but come with different twist distributions not only in jig (lower part) but also in flight shape (middle part). This twist difference in flight shape reflects the automatically applied adjustments to meet the target lift distributions from Fig. 10. For example, the flight shape twist of the study aircraft with the bell-shaped lift distribution (solid light grey line in the middle part) is decreased in the outboard region to reach the locally required low lift values.

To analyze the impact of the different lift distributions and their influence on the wing dimensioning process on the overall aircraft design level, Fig. 12 shows changes in key parameters for each converged aircraft compared to the reference aircraft.

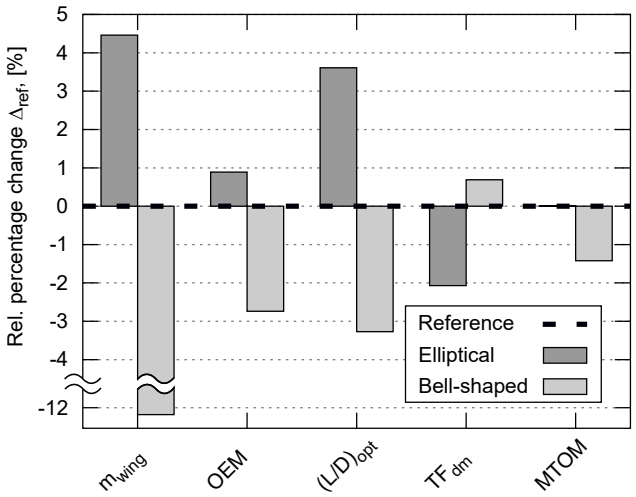

FIG 12. Key parameter changes compared to ref. aircraft

For the elliptical lift distribution, a strong outboard loading and the resulting increased root bending moment leads to an increase in wing mass of $\Delta \mathrm{m_{wing}} \approx 4.5\,\%$; combined with the snowball effect captured in MICADO, this results in an increase of the operating empty mass of $\Delta \mathrm{OEM} \approx 1.0\,\%$. However, the improved aerodynamics outbalance these detrimental mass effects, resulting in a decreased trip fuel consumption of $\Delta \mathrm{TF}_{2943\,\mathrm{NM}} \approx -2.0\,\%$ while keeping the maximum take-off mass almost constant.

The strong inboard loading and the associated decreased root bending moment of the bell-shaped lift distribution leads to a significant decrease in wing mass of $\Delta \mathrm{m_{wing}} \approx -12.3\,\%$. Even though this is partly transferred to the MTOM, the detrimental effects on the aerodynamics $(\Delta(\mathrm{L/D})_{\mathrm{opt}} \approx -3.3\,\%)$ result in an increase in trip fuel of $\Delta \mathrm{TF}_{2943\,\mathrm{NM}} \approx 0.7\,\%$.

Without going into an extensive analysis of the occurring aerodynamic and structural effects, this study demonstrated that—contrary to semi-empirical handbook methods—the more detailed wing mass estimation correctly maps the significant impact of different lift distributions on the overall aircraft design parameters. Thereby, it enhances the capabilities of MICADO since such sensitivity studies no longer neglect aerostructural effects.

4. CONCLUSION AND OUTLOOK

This work presents a new MICADO tool developed based on existing methods from the literature. It enables a more detailed wing mass estimation in MICADO and allows for mapping aerostructural interactions. Whereas the analysis of the impact of different lift distributions demonstrates the new capabilities within MICADO, the results from the first application study suggest that—for the reference aircraft used in this work—a more detailed consideration of different flight shapes during a mission is not necessary for the conceptual design context. Another study shows that an aircraft with a VC application has slight variations in flight shape with deployed flaps compared to a rigid wing configuration. However, these differences are negligible from both aerodynamic and mission perspectives. In future studies, the conducted analyses will be repeated for different aircraft range types. The suggested design guidelines can be assessed and eventually generalized from these studies. For larger aircraft, however, using a simplified linear FEM is not recommended; implementing non-linear FEM methods is part of current work at ILR.

ACKNOWLEDGMENTS

The research presented in this publication has been conducted within the frameworks of the CATeW (Couple Aerodynamic Technologies for Aircraft Wings) and the H2Avia (Hydrogen in Aviation) projects and has received funding from the Federal Aviation Research Programmes LuFo VI.1 and VI.2, respectively. We want to acknowledge the support of the Federal Ministry for Economic Affairs and Climate Action and the project partners for the valuable discussions. In addition, we thank all involved (former) colleagues and student assistants at ILR. We greatly appreciate the work of Dimitri Wecker in his bachelor's thesis, in which he developed the initial version of the presented new MICADO module.

Contact address:

tim.effing@ilr.rwth-aachen.de

References

[1] K. Risse, E. Anton, T. Lammering, K. Franz, and R. Hörnschemeyer. An Integrated Environment for Preliminary Aircraft Design and Optimization. In AIAA, editor, *53rd AIAA/ASME/ASCE/AHS/ASC Structures, Structural Dynamics and Materials Conference*, 2012. DOI: 10.2514/6.2012-1675.

[2] F. Schültke, B. Aigner, T. Effing, P. Strathoff, and E. Stumpf. MICADO: Overview of Recent Developments within the Conceptual Aircraft Design and Optimization Environment. In Deutsche Gesellschaft für Luft- und Raumfahrt - Lilienthal - Oberth e.V., editor, *69. Deutscher Luft- und Raumfahrtkongress*. Bonn, Germany, 2020. DOI: 10.25967/530093.

[3] F. Schültke and E. Stumpf. UNICADO - Development and Establishment of a University Conceptual Aircraft Design Environment. In Deutsche Gesellschaft für Luft- und Raumfahrt - Lilienthal - Oberth e.V., editor, *69. Deutscher Luft- und Raumfahrtkongress*, 2020. DOI: 10.18154/RWTH-2021-04203.

[4] F. Peter, K. Risse, F. Schültke, and E. Stumpf. Variable Camber Impact on Aircraft Mission Planning. In *53rd AIAA Aerospace Sciences Meeting 2015*. Curran, Red Hook, NY, 2015. DOI: 10.2514/6.2015-1902.

[5] K. Risse. *Preliminary Overall Aircraft Design with Hybrid Laminar Flow Control*. Ph.D. thesis, RWTH Aachen University, Aachen, Germany, 2016. DOI: 10.18154/RWTH-2017-00974.

[6] R. Stephan, N. Schneiders, F. Schültke, F. Peter, and E. Stumpf. Evaluation of a Distributed Variable-Camber Trailing-Edge Flap System at Preliminary Aircraft Design Stage. In AIAA, editor, *AIAA AVIATION 2022 Forum*, Reston, VA, 2022. DOI: 10.2514/6.2022-3519.

[7] T. Effing, V. Schmitz, F. Schültke, F. Peter, and E. Stumpf. Combined Application of Hybrid Laminar Flow Control and Variable Camber in Preliminary Aircraft Design. In *Proceedings of the 33rd Congress of the International Council of the Aeronautical Sciences*, Stockholm, Sweden, 2022. DOI: 10.18154/RWTH-2022-11091.

[8] J. Thorbeck. Manuskript zur integrierten Lehrveranstaltung Flugzeugentwurf I und II. Institute of Aeronautics and Astronautics, Technical University Berlin, Berlin, Germany, 2003.

[9] D. Howe. *Aircraft Conceptual Design Synthesis*. Professional Engineering Publishing, London and Bury St Edmunds, United Kingdom, 2010. DOI: 10.1002/9781118903094.

[10] K. Seywald. *Wingbox Mass Prediction considering Quasi-Static Nonlinear Aeroelasticity*. Diploma thesis, 2011. https://api.semanticscholar.org/CorpusID:92994105.

[11] Z. Wan, L. Liang, and C. Yang. Method of the Jig Shape Design for a Flexible Wing. *Journal of Aircraft*, 51(1):327–330, 2014. DOI: 10.2514/1.C031926.

[12] T. A. Zeiler. Divergence and Convergence of Iterative Static Aeroelastic Solutions. *Journal of Aircraft*, 36(4):716–718, 1999. DOI: 10.2514/2.2495.

[13] F. Hürlimann. *Mass Estimation of Transport Aircraft Wingbox Structures with a CAD/CAE-Based Multidisciplinary Process*. Ph.D. thesis, ETH Zurich, Zurich, Switzerland, 2010. DOI: 10.3929/ethz-a-006361295.

[14] D. Wecker. *Entwicklung einer Methode zur Berücksichtigung aeroelastischer Effekte im Flugzeugvorentwurf*. Bachelor thesis, RWTH Aachen University, Aachen, Germany, 2015. https://publications.rwth-aachen.de/record/971147.

[15] M. Drela and H. Youngren. AVL 3.40 User Primer. Massachusetts Institute of Technology (MIT), Cambridge, MA, 2022, https://web.mit.edu/drela/Public/web/avl.

[16] CeRAS. Central Reference Aircraft data System. Institute of Aerospace Systems (ILR), RWTH Aachen University, Aachen, Germany, https://ceras.ilr.rwth-aachen.de.

[17] K. Risse, K. Schäfer, F. Schültke, and E. Stumpf. Central Reference Aircraft data System (CeRAS) for research community. *CEAS Aeronautical Journal*, 7(1):121–133, 2016. DOI: 10.1007/s13272-015-0177-9.

[18] T. Effing, F. Peter, E. Stumpf, and M. Hornung. Approach for the Aerodynamic Optimization of the Twist Distribution of Arbitrary Wing Geometries on Conceptual Aircraft Design Level. In Deutsche Gesellschaft für Luft- und Raumfahrt - Lilienthal - Oberth e.V., editor, *70. Deutscher Luft- und Raumfahrtkongress*, 2021. DOI: 10.25967/550197.